Zn-containing immature structure of a Rieske-type iron-sulfur protein

Iron-sulfur clusters are involved in a wide range of biological processes, including enzymatic reactions, photosynthesis, and respiration, as prosthetic groups for various proteins. Iron-sulfur clusters are biosynthesized by protein machinery, such as sulfur mobilization (SUF) and iron-sulfur cluster (ISC) systems [1]. The biosynthesis of iron-sulfur clusters is divided into two main steps: assembly and insertion (Fig. 1(a)). In the assembly step, iron-sulfur cluster assembly is catalyzed by cysteine desulfurases on scaffold proteins. The iron-sulfur clusters are transferred to the final target proteins in the next insertion step with the assistance of molecular chaperones. The bacterial ISC system is similar to the mitochondrial ISC system and the central component proteins are homologous to each other [2]. Although the elucidation of the assembly step has recently progressed [3], the insertion step from scaffold proteins to the target protein remains unclear. Accordingly, the molecular details of iron-sulfur protein maturation remain unclear.

The Rieske protein PetA is a subunit of the bacterial cytochrome bc_1 complex [4]. PetA is composed of a single transmembrane α-helix and one soluble globular domain with a Rieske-type [2Fe–2S] cluster (Fig. 1(b)). In this study [5], the soluble domain of PetA from a photosynthetic bacterium was expressed in *Escherichia coli* cells. In a purification process with size-exclusion chromatography (SEC), PetA was divided into a colorless elution peak of approximately 40 kDa, corresponding to the dimer, and a dark-brown peak of approximately 20 kDa, corresponding to the monomer (Fig. 2(a)). The ultraviolet-visible (UV-vis) absorption spectra indicated that only the monomer fraction contained iron-sulfur clusters. Therefore, the dimer and monomer fractions in the SEC were assigned to the immature and mature forms of PetA, respectively.

The crystals of the two PetA samples were obtained and used for X-ray diffraction (XRD) measurements at SPring-8 **BL41XU**. The immature PetA structure was determined at 1.7 Å resolution, whereas that of [2Fe–2S]-containing mature PetA was determined at 1.8 Å resolution. The structures of both forms were typical of the Rieske subunit of the cytochrome bc_1 complex. In immature PetA, $ZnCl_2$ is found in the cluster-binding site instead of [2Fe–2S] (Fig. 2(b)). The zinc ion is chelated in a tetra-coordination geometry by two cysteine residues (Cys124 and Cys152) and two chloride ions. Only one histidine residue (His155) exhibited a conformational difference in the cluster-binding site (Figs. 2(b,c)), whereas no significant differences were observed between the two structures. This implies that the structure of the cluster-binding site was almost completely constructed prior to the insertion of [2Fe–2S].

To investigate the oligomeric structure of Zn-PetA in solution, a SEC coupled with small-angle X-ray scattering (SEC–SAXS) experiments were performed at SPring-8 **BL38B1** (Fig. 3(a)). An *ab initio* envelope model derived from the SAXS data had the following approximate dimensions: 80 × 40 × 40 Å^3 (Fig. 3(b)). The scattering curve calculated from one of the dimers formed in the crystal fit the experimental scattering data better than those of the other dimers in the crystal (Fig. 3(a)). The two protomers in the dimer were related to translational symmetry. In the dimer model, the hydrophobic patch of one protomer interacted with the hydrophobic patch of another protomer. Furthermore, a salt bridge was formed between the two protomers. The residues involved in these interactions were highly conserved in bacterial

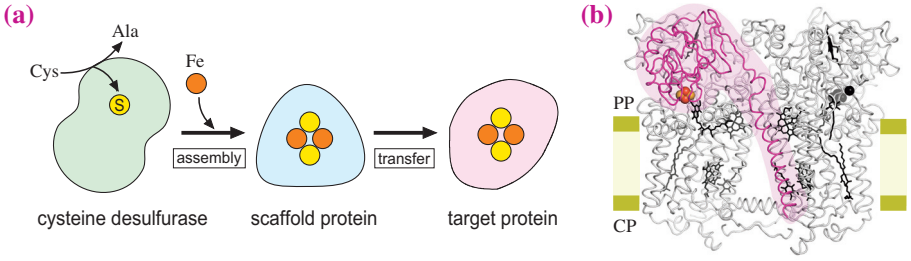

Fig. 1. Biosynthesis of iron-sulfur clusters. (**a**) The ISC system. (**b**) PetA in the cytochrome bc_1 complex of a photosynthetic bacterium [4]. The complex contains two PetA, one of those is colored in magenta. PP: periplasmic side, CP: cytoplasmic side.

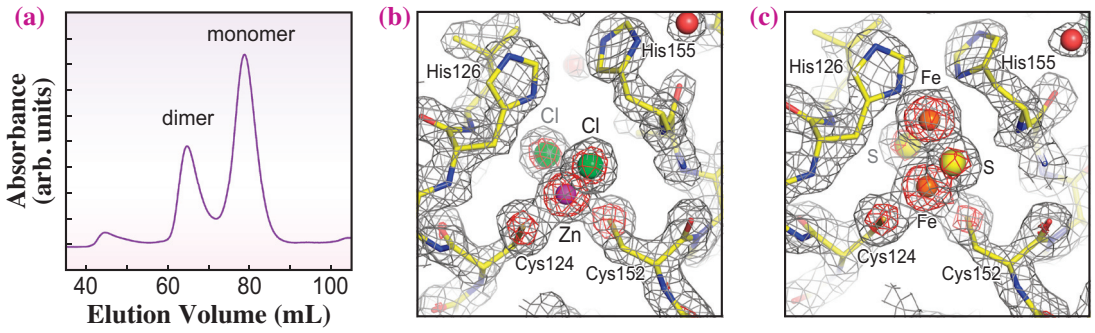

Fig. 2. Structural analyses of PetA. (**a**) The SEC elusion profile monitored at 280 nm. (**b**) Electron density ($2F_{obs} - F_{calc}$) map for the cluster-binding site of Zn-PetA. (**c**) Electron density map for [2Fe–2S]-PetA.

PetA. Thus, such dimer can be formed in bacterial PetA. When structural changes are introduced in the C-terminal region of one protomer, the fit to the envelope are further improved (Fig. 3(b)). These changes can inhibit the formation of salt bridges between the dimer and another protomer. This should explain why they did not form oligomers larger than dimers. Iron-sulfur clusters were confirmed to be reconstituted in Zn-PetA under *in vitro* condition [5]. This indicates that the Zn-containing structure determined in this study is an immature structure that appears before the maturation of iron-sulfur cluster-containing proteins. The dimerization of immature proteins may avoid unfavorable degradation caused by proteases in cells.

In this study, the combination of X-ray crystallography and SAXS analysis revealed the tertiary and quaternary structures of the immature form of a Rieske-type iron-sulfur protein to be accurately elucidated. Further studies should be performed to reveal the insertion process in detail, including the formation of intermediate complexes of the scaffold protein and the target protein.

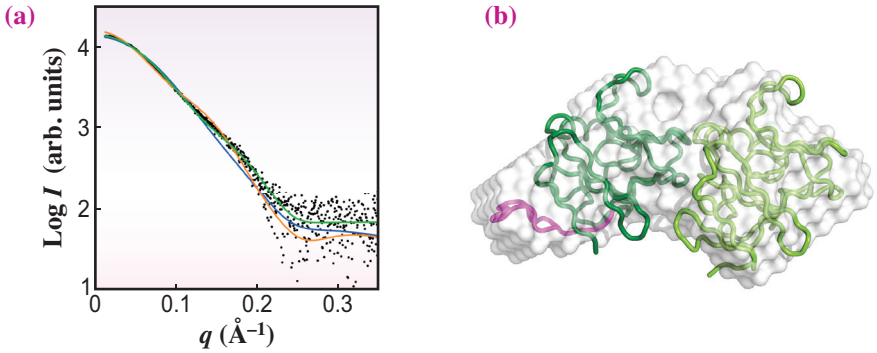

Fig. 3. SAXS analysis for the dimer structure of Zn-PetA. (**a**) The experimental scattering data are shown as black dots, and the calculated curves of three dimer candidates constructed based on the crystal packing are shown in green, orange and blue. (**b**) The *ab initio* envelope model derived from the SAXS data is represented as gray surface. The most plausible dimer model giving the green curve in the (a) is fitted to the envelope. The changed portion of the C-terminus is colored in magenta.

Kazuki Takeda

Department of Chemistry, Kyoto University

Email: ktakeda@kuchem.kyoto-u.ac.jp

References

[1] J. J. Braymer *et al.*: BBA Mol. Cell Res. **1868** (2021) 118863.
[2] C. Baussier *et al.*: Adv. Microb. Physiol. **76** (2020) 1.
[3] B. Srour et *al.*: J. Am. Chem. Soc. **144** (2022) 17496.
[4] L. Esser *et al.*: J. Biol. Chem. **283** (2008) 2846.
[5] *E. Tsutsumi, S. Niwa, R. Takeda, N. Sakamoto, K. Okatsu, S. Fukai, H. Ago, S. Nagao, H. Sekiguchi, K. Takeda: Commun. Chem.* ***6*** *(2023) 190.*